

Review

# Current Research Studies of Mg–Ca–Zn Biodegradable Alloys Used as Orthopedic Implants—Review

Bogdan Istrate <sup>1</sup>, Corneliu Munteanu <sup>1,2,\*</sup>, Iulian-Vasile Antoniac <sup>3,4,\*</sup> and Ștefan-Constantin Lupescu <sup>5</sup>

<sup>1</sup> Faculty of Mechanical Engineering, “Gheorghe Asachi” Technical University of Iasi, 63 D Mangeron Blvd, 700050 Iasi, Romania

<sup>2</sup> Technical Science Academy Romania, 26 Dacia Blvd, 030167 Bucharest, Romania

<sup>3</sup> Faculty of Materials Science & Engineering, Politehnica University of Bucharest, 313 Splaiul Independentei, Dist 6, 060042 Bucharest, Romania

<sup>4</sup> Academy of Romanian Scientists, 54 Splaiul Independentei Street, District 5, 050094 Bucharest, Romania

<sup>5</sup> Department of Mechanics and Technologies, Stefan cel Mare University of Suceava, 13 University Street, 720229 Suceava, Romania

\* Correspondence: corneliu.munteanu@academic.tuiasi.ro (C.M.); antoniac.iulian@gmail.com (I.-V.A.)

**Abstract:** Biodegradable alloys and especially magnesium-based alloys are considered by many researchers as materials to be used in medicine due to their biocompatibility and excellent mechanical properties. Biodegradable magnesium-based materials have applications in the medical field and in particular in obtaining implants for small bones of the feet and hands, ankles, or small joints. Studies have shown that Mg, Zn, and Ca are found in significant amounts in the human body and contribute effectively and efficiently to the healing process of bone tissue. Due to its biodegradability, magnesium alloys, including Mg–Ca–Zn alloys used in the manufacture of implants, do not require a second surgery, thus minimizing the trauma caused to the patient. Other studies have performed Mg–Ca–Zn system alloys with zinc variation between 0 and 8 wt.% and calcium variation up to 5 wt.%, showing high biocompatibility, adequate mechanical properties, and Mg<sub>2</sub>Ca and Mg<sub>6</sub>Ca<sub>2</sub>Zn compounds in microstructure. Biocompatibility is an essential factor in the use of these materials, so that some investigations have shown a cell viability with values between 95% and 99% compared with the control in the case of Mg–0.2Ca–3Zn alloy. In vivo analyses also showed no adverse reactions, with minimal H<sub>2</sub> release. The aim of this review includes aspects regarding microstructure analysis and the degradation mechanisms in a specific environment and highlights the biocompatibility between the rate of bone healing and alloy degradation due to rapid corrosion of the alloys.

**Keywords:** Mg–Ca–Zn biodegradable alloys; microstructure; corrosion; biocompatibility



**Citation:** Istrate, B.; Munteanu, C.; Antoniac, I.-V.; Lupescu, Ș.-C. Current Research Studies of Mg–Ca–Zn Biodegradable Alloys Used as Orthopedic Implants—Review. *Crystals* **2022**, *12*, 1468. <https://doi.org/10.3390/cryst12101468>

Academic Editor: Pavel Lukáč

Received: 20 September 2022

Accepted: 14 October 2022

Published: 17 October 2022

**Publisher’s Note:** MDPI stays neutral with regard to jurisdictional claims in published maps and institutional affiliations.



**Copyright:** © 2022 by the authors. Licensee MDPI, Basel, Switzerland. This article is an open access article distributed under the terms and conditions of the Creative Commons Attribution (CC BY) license (<https://creativecommons.org/licenses/by/4.0/>).

## 1. Introduction

Biomaterials have a large scale of applications, especially in the medical domain, and are exposed in direct or indirect contact with a biological medium [1]. The most important aspect of a biomaterial is the biocompatibility, which is defined as “the ability of a material to function with an appropriate host response in a specific application” [2].

Unlike conventionally inert biomaterials, these types of biomaterials promote beneficial interactions with implantation sites. Biodegradable materials are among the most beneficial biomaterials due to the fact that they aid the healing process of the affected tissue during the gradual healing process. Five years ago, the global market of materials used in medicine was set at approximately USD 83 billion and is likely to expand to over USD 215 billion by 2024, having an annual growth rate of approximately 15% during the specified period [3,4].

Magnesium (Mg) is an abundant chemical element in the human body that plays a crucial role in cellular metabolism, membrane function, and membrane integrity [5].

Magnesium is required by every enzyme system involved in DNA processing [5]. Internal cell cycle and apoptosis are also influenced by magnesium [5].

Mg and its alloys are used very often as biodegradable bone implants and stents because of their very good physical and mechanical properties, such as excellent biocompatibility, high strength, and low Young's modulus [6–9]. The advantages/disadvantages of biodegradable magnesium-based alloys are presented in Figure 1. However, the fast degradation rate of Mg alloys prevents implants from performing their surgical function before being extracted; inhomogeneous local corrosion starting from the surface of Mg alloys makes the corrosion behavior uncontrollable. Additionally, a significant amount of hydrogen accumulates in gas pockets by the corroding Mg implant, which will delay the healing of the surgical region and lead to an inflammatory reaction.

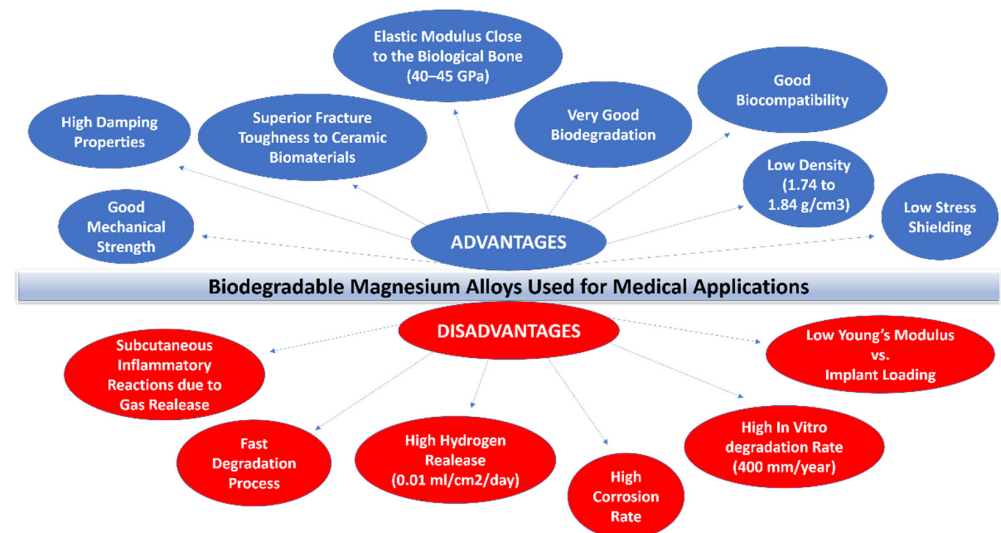


**Figure 1.** Main aspects of biodegradable magnesium alloys used in the medical domain [10].

There are multiple publications available in the state of art of the research presenting the microstructural characterization, mechanical characteristics, electrochemical behavior, and biocompatibility evaluation through in vitro and in vivo studies of these biodegradable materials used for orthopedic purposes [8]. Thus, depending on the desired specific implant, Mg-based alloys can be classified into several systems, as shown in Figure 2.

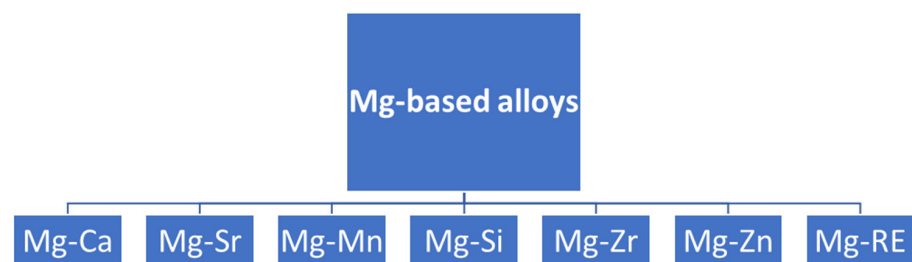


**Figure 2.** Classification of magnesium-based alloys [8].

Calcium (Ca) is one of the most desired alloying elements for biodegradable alloys. It is one of the most abundant minerals in human bones [11] and is necessary for human bone growth. It is also a necessary element in chemical signaling with cells [12]. Mg–Ca is basically made up of two phases,  $\alpha$ -Mg and  $Mg_2Ca$ . An intermetallic phase, such as  $Mg_2Ca$ , refines the Mg microstructure and strengthens the alloy.

Zinc (Zn) exhibits a refinement property for the microstructure, thus increasing the mechanical strength of magnesium [13]. Mg–Zn biodegradable alloys have proved improved electrochemical results in standard biological mediums compared with pure magnesium,

which has been attributed in part to zinc's capability to form Ni- and Fe-containing compounds [14].

Zn, unlike other alloying elements, which are not suitable for alloying, is a necessary trace element for the human body. Mg–Zn alloys are made up primarily of an a-Mg matrix and a c-MgZn phase, with a solubility limit of 6.2 wt.% for Zn in magnesium [15]. Zn raises YS from 1 to 6 wt.% when added to Mg, as expected. The maximum UTS (216.8 MPa) and elongation (15.8%) may be attained if the Zn concentration is kept to 4 wt.% [15]. The addition of Ca, Zr, Sr, Y, Mn, and Si to Mg–Zn-based alloys has been studied extensively [16,17] to enhance the mechanical characteristics by refining the microstructure or producing distinct structures. Ca is a powerful grain refiner in magnesium-based alloys, as previously stated. However, the maximum Ca solubility in Mg is just 1.34 wt.%. Above 1 wt.%, Ca decreases the strength and ductility of magnesium-based alloys [18]. If more than 0.5 wt.% Ca is added to Mg–4Zn-based alloys, the UTS and ductility decrease [15].

Additionally, Mg–Zn–Ca alloys, with Ca added as a third element, have been shown to have enhanced biocompatibility. A 2–5 h of age hardening improves mechanical properties, and corrosion is reduced by half from the original estimate [19]. Mechanical qualities are improved in Mg–4.0Zn–0.2Ca ternary alloys (as cast and extruded), with a tensile yield strength of 240 MPa, an ultimate tensile strength of 297 MPa, and an elongation of 21.3%. After 30 days in a SBF solution, YTS, UTS, and elongation are 160 MPa, 220 MPa, and 8.5%, respectively, indicating high biocompatibility and a lowered degradation rate.

The objective of the present paper is to detail the aspects regarding Zn and Ca influence in magnesium-based alloys in order to observe the main properties. The originality of this review also includes aspects regarding microstructure analysis and the degradation mechanisms in specific environment and highlights the biocompatibility between the rate of bone healing and alloy degradation due to rapid corrosion of the alloys.

## 2. Alloying Element Selection in Mg-Based Alloys for Orthopedic Implants

Pure Mg is not very often used in the biomedical domain. Magnesium, as a chemical element, presents significant improvement of physicochemical properties by alloying with other different elements. These elements provide grain refinement, precipitation hardening, and solid solution hardening. Commercial cast magnesium alloys are mainly classified into Mg–Ca-, Mg–Zn-, Mg–Al-, Mg–Mn-, Mg–Zr- and Mg–RE-based alloys [20]. However, biocompatibility, improved mechanical properties, and improved degradation rate must take into account the careful selection of alloying elements in Mg alloys for orthopedic implants. High biocompatibility and good mechanical properties correlated with the degradation rate represent the main goal requirements of Mg-based biodegradable alloys (Figure 3). For improving these characteristics, researchers have approached two main directions: alloying and surface depositions. The most common nutritional alloying elements used in biodegradable Mg alloys for orthopedic implants include calcium (Ca), zinc (Zn), manganese (Mn), strontium (Sr), tin (Sn), silver (Ag), and RE elements [21].

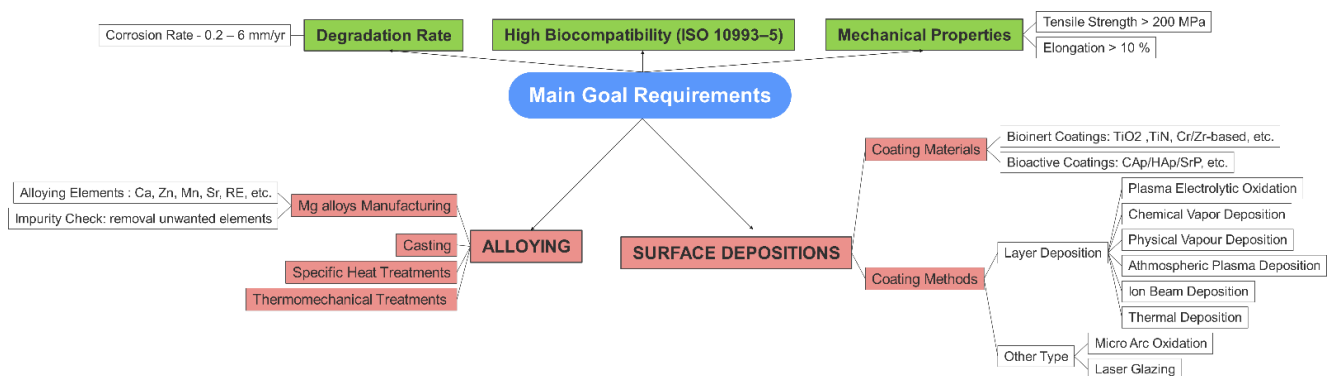
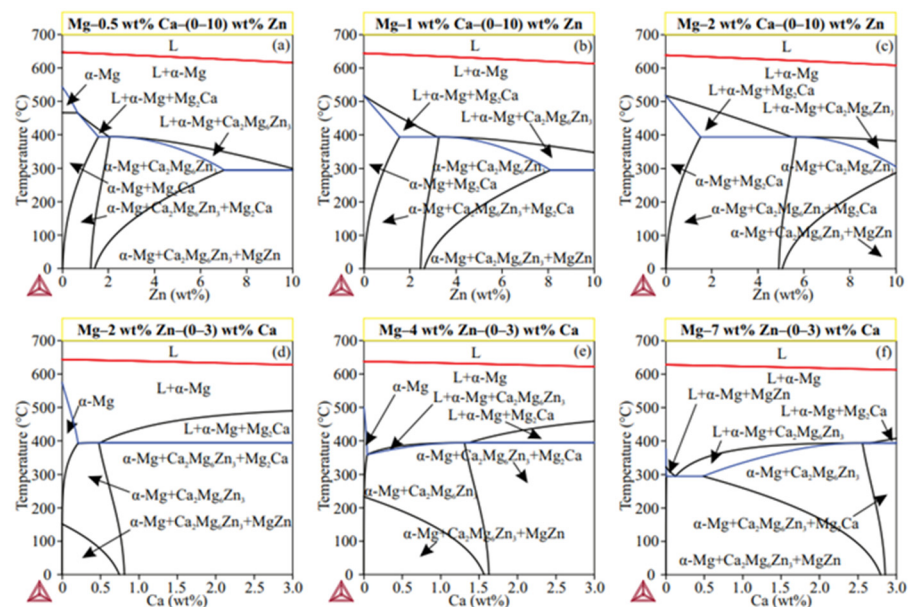


Figure 3. Main goal requirements of Mg-based alloys [22–24].

Due to the fact that Ca is one of the basic components of the human body, it contributes to many essential functions. At the same time, Ca is stored in the highest quantity in bones and teeth and contributes to the process of osseointegration. Thus, studies have confirmed that the introduction of calcium into magnesium has a positive effect on bone healing [25]. From a metallographic point of view, Ca refines the microstructure and contributes to increase the mechanical strength and creep properties of Mg by forming stable intermetallic compounds. Furthermore, acid etching is an effective surface treatment method to adapt the biomineralization and degradation behaviors of Mg–Ca alloy to the physiological environment [26]. Nidadavolu et al. [27] conducted a powder metallurgy (PM) technique on samples of the biodegradable Mg–0.6Ca system with varied porosities. The researchers found that one large pore occupies a significant percentage of the measured pore volume in Mg–0.6Ca samples with 21% porosity. This shows that porous Mg alloy pores are very dependent on each other. As an important trace element, Zn is linked in many biological mechanisms, such as immune response, carbohydrate catabolism, wound healing, bone development, and growth [28]. The necessary amount of Zn for children and adults is about 2 mg/day and 6.5–15 mg/day [29]. Additionally, more than 85% of Zn is stored in the muscle and bone. Being another biodegradable metal, the degradation rate of Zn is slower than the Mg degradation rate, but faster than that of Fe [30]. Zn improves the yield and ultimate strength of Mg alloy implants, depending on the Zn concentration [31].

Bazhenov et al. [32] present in Figure 4 the polythermal cross sections of Mg–Zn–Ca phase diagrams calculated using the Thermo-Calc software. The liquidus and solidus lines are highlighted distinctly. After solidification, magnesium containing up to 10 wt.% Zn and 3 wt.% Ca showed  $\alpha$ -Mg,  $Mg_2Ca$ ,  $Ca_2Mg_6Zn_3$ , and MgZn as main phases. With an increase in Ca and Zn content, the liquidus temperature of the alloys also remained almost constant; however, the solidus temperature decreased significantly. For example, at Zn contents >7 wt.%, the solidus temperature was 295 °C due to low-melt-formation-phase MgZn.



**Figure 4.** Polythermal cross sections of Mg–Zn–Ca phase diagrams calculated: (a) Mg–0.5 wt.% Ca–(0–10) wt.% Zn; (b) Mg–1 wt.% Ca–(0–10) wt.% Zn; (c) Mg–2 wt.% Ca–(0–10) wt.% Zn; (d) Mg–2 wt.% Zn–(0–3) wt.% Ca; (e) Mg–4 wt.% Zn–(0–3) wt.% Ca; (f) Mg–7 wt.% Zn–(0–3) wt.% Ca. Reprinted with permission from Ref. [32].

Wasiur-Rahman [33] shows in Figure 5 that the ternary Mg–Ca–Zn system has 6 ternary eutectic points (E1–E6), 11 quasi-peritectic points (U1–U11), 1 ternary peritectic point (P1), and 8 maximum points (m1–m8) present in this system. This was based on calculations by Paris [34], who reported two different compounds, namely,  $CaZn_{10}$  and  $CaZn_4$ , in this region.

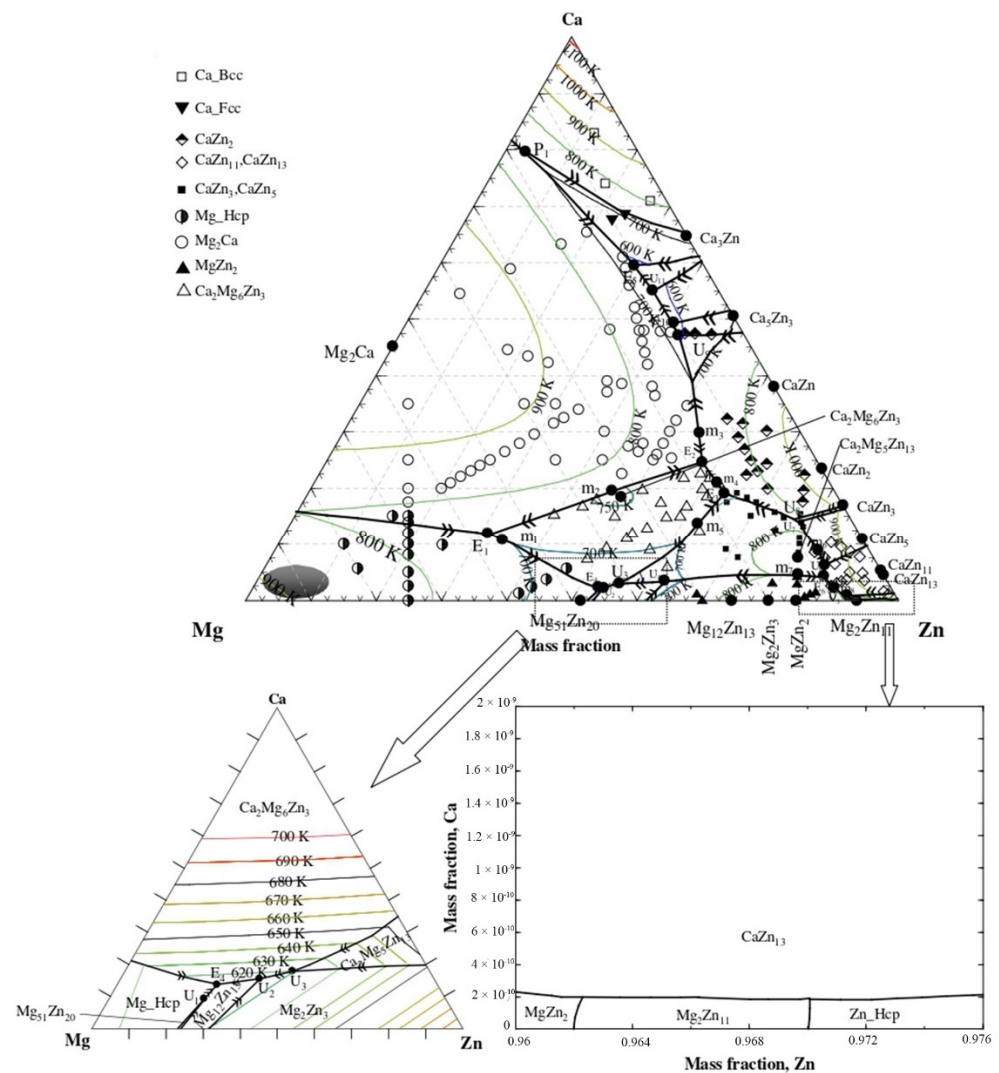
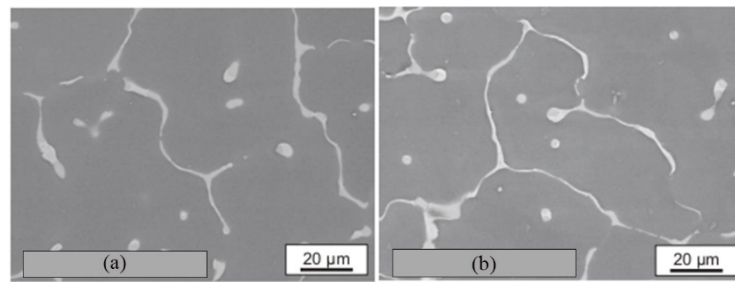


Figure 5. Mg–Zn–Ca ternary diagram. Reprinted with permission from Refs. [33,34].

More research revealed four additional compounds, which were classified as  $\text{CaZn}_3$ ,  $\text{CaZn}_5$ ,  $\text{CaZn}_{11}$ , and  $\text{CaZn}_{13}$ . Therefore, in Figure 5, a common symbol is used to indicate  $\text{CaZn}_3$  and  $\text{CaZn}_5$ , while another symbol is used to highlight  $\text{CaZn}_{11}$  and  $\text{CaZn}_{13}$ , based on the work performed by Paris [34]. Additionally, the occurrence of a second ternary compound,  $\text{Ca}_2\text{Mg}_5\text{Zn}_{13}$ , has been reported by both Paris [34] and Clark [35].

These properties are supported by studies [36], which found that ternary alloys with 1.8 wt.% zinc had coarser grains than those with 0.8 wt.% zinc. Magnesium–zinc reflections were fully characterized by X-ray analyses performed by [36] with  $\text{Mg}_2\text{Ca}$ ,  $\text{MgZn}_2$ , and  $\text{Mg}_6\text{Ca}_2\text{Zn}_3$  as compounds for the ternary alloys. In Figure 6 are presented some SEM images of some Mg–Ca–Zn as-cast alloys.



**Figure 6.** SEM images of some Mg–Ca–Zn as-cast alloys: (a) Mg-1.6Ca-0.8Zn; (b) Mg-1.6Ca-1.8Zn [36].

### 3. Physicochemical and Mechanical Properties

#### 3.1. Microstructural Properties

Gong et al. [37] studied Mg–Ca–Zn alloys' microstructure with high Zn content (between 0% and 7.5% Zn). Increasing Zn content leads to decreasing grain sizes. Correlated also with studies conducted by Zhang [38], in the solidification process, with decreasing temperature, the solubility of Zn and Ca elements in the Mg matrix decreases sharply, and a large amount of Ca and Zn enriches at the leading edge of the solid–liquid interface. Figure 7 highlights the microstructural aspects of Mg–Ca–Zn alloys, elaborated by Gong et al. [37]. X-ray diffraction results correlated with the microstructure highlight the Mg<sub>2</sub>Ca eutectic and the α-Mg solid solution. With increasing Zn content to 2%, the Ca<sub>2</sub>Mg<sub>6</sub>Zn<sub>3</sub> phase appears. In the case of the alloy XZ15 (4.7% Zn), here, only the diffraction peaks of the α-Mg and Ca<sub>2</sub>Mg<sub>6</sub>Zn<sub>3</sub> phases are detected, while the diffraction peaks of the Mg<sub>2</sub>Ca phase disappear. When the Zn content is further increased to 8%, a new diffraction peak of the Ca<sub>2</sub>Mg<sub>5</sub>Zn<sub>13</sub> phase appears [37].

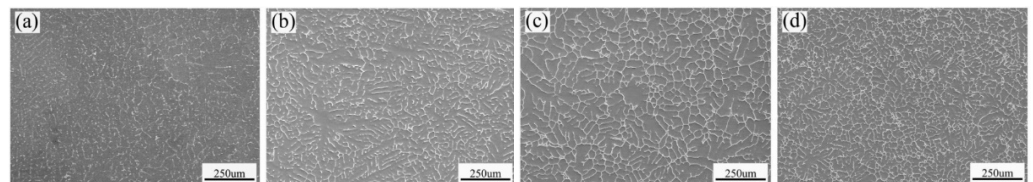


**Figure 7.** SEM images of the as-cast Mg–Ca–Zn alloys: (a) XZ10, (b) XZ12, (c) XZ15, (d) XZ18 [37].

Pulido-González et al. presented the effects of heat treatments on Mg-1 wt.% Zn-1 wt.% Ca (ZX11) and Mg3 wt.% Zn-0.4 wt.% Ca (ZX30) alloys, which consisted of heating at 450 °C for 24 h, quenching and ageing at 180 °C [39]. Microstructure analysis, mechanical behavior, and biocorrosion aspect (Hank's immersion solution) were evaluated in both alloys (cast and solution treatment conditions). From these studies, the following conclusions can be drawn: (i) after solidification, both alloys show a microstructure composed of α-Mg grains separated by Mg<sub>2</sub>Ca and Ca<sub>2</sub>Mg<sub>6</sub>Zn<sub>3</sub> precipitates in ZX11 alloy and only by Ca<sub>2</sub>Mg<sub>6</sub>Zn<sub>3</sub> precipitates in ZX30 alloy; (ii) solution treatment leads to complete dissolution of the Ca<sub>2</sub>Mg<sub>6</sub>Zn<sub>3</sub> phase in ZX11 alloy, but to a low degree of dissolution of this phase in ZX30 alloy.

Zander et al. investigated the microstructure of several Mg–Ca–Zn biodegradable alloys, modifying the percentages of Ca (0.6 to 1.6 wt.%) and Zn (0.8 to 1.8 wt.%). In the Mg–0.6Ca system, alloying with 0.8% zinc results in a little grain refinement from 67 ± 5 microns to 56 ± 8 microns. Ternary alloys with Zn concentrations more than 1.8 wt.% have a grain microstructure with bigger grains than alloys with Zn values of 0.8 wt.%. The average grain size is increased by 21% for Mg–1.6Ca–xZn and by 32% for Mg–0.6Ca–xZn (x = 0.8, 1.8 wt.%) compared with Mg–0.6 Ca alloys [36]. If calcium content is increased from 0.6 to 1.6 wt.%, a coarser, more dendritic microstructure and an average increase in grain size are seen at 22% for Mg–xCa–1.8Zn and at 23% for Mg–xCa–0.8Zn. This demonstrates that second compounds are present not only on grain boundaries, but also in interdendritic interstices.

### 3.2. Mechanical Properties

The most benefits of magnesium-based alloys are their biodegradability, biocompatibility, and good mechanical properties [40]. They are considered to be the third category of biomaterials after stainless steels, Co–Cr alloys, and Ti alloys [41,42].

Mg orthopedic implants have elastic modulus close to that of biological bone, while the ultimate tensile strength (UTS) of magnesium is higher than that of ceramic biomaterials. However, the implant must present its load without any deformation.

In order to design a suitable medical implant, it is necessary to analyze its degradation rate, which should be in a controlled manner. The effect of stress shielding is also related to the degradation rate, because as the degradation period of the implant material passes, the load may gradually shift to the bone tissue [43].

Zn has a high solubility in Mg (6.2 wt.%), which makes it an important alloying element. Because of its solid solution strengthening and age strengthening action, it helps the alloy keep its mechanical characteristics over time. The ultimate tensile strength and elongation of as-cast Mg–Zn alloys increased significantly with increasing Zn concentrations up to 4 wt.%, but beyond that point, both characteristics decreased [15] along with the alloy's corrosion resistance.

In order to present the importance of Zn, in Table 1 are highlighted the mechanical properties of some biodegradable biomaterials in comparison with classical biomaterials.

**Table 1.** Mechanical properties of some biodegradable biomaterials in comparison with classical biomaterials.

Materials	Density (g/cm <sup>3</sup> )	Young's Modulus (MPa)	Ultimate Strength (MPa)	Yield Strength (MPa)	Elongation (%)	Hardness (HV)	Ref.
Bone	1.8–21	15–25	110–130	104–121	0.7–3	-	[44]
Magnesium	1.75	41–45	95–185	65–95	2–10	-	[45]
Calcium	1.54	17	110	-	-	-	[46]
Zinc	5.4	9	33	-	16	18	[47]
SS316L stainless steel	7.95	200	490	190	40	-	[48]
Ti-6Al-4V titanium alloys	4.4	114	950	880	14	-	[49]
CoCr20Ni15Mo7–Co–Cr alloys	7.8	195–230	450–960	240–450	50	-	[50]
Mg-1Ca	-	-	71	40	1.87	-	[18]
Mg-3Ca	-	-	-	136	1.9	-	[51]
Mg-1Zn	-	-	134	25	18.5	-	[52]
Mg-5Zn	-	-	195	76	8.5	53.8	[13]
Mg-7Zn	-	-	136	67	6	56.2	[53]
Mg-4Zn-0.2Ca	-	-	255	58	17.5	-	[54]
Mg-4Zn-0.5Ca-0.16Mn	-	-	180	175	0.2	70	[55]
Mg-1.2Zn-0.5Ca	-	-	116–126	57–63	3–3.3	45	[19]
Mg-23Zn-5Ca	2.84	50.38	-	-	-	-	[56]
Mg-1Zn-1Ca	-	43.9	125	45	5.7	-	[57]
Mg-2Zn-1Ca	-	44.7	143	52	7.3	-	[57]
Mg-3Zn-1Ca	-	45.3	160	57	8.3	-	[57]
Mg-4Zn-1Ca	-	45.9	182	63	9.1	-	[57]
Mg-5Zn-1Ca	-	45	173	65	8.2	-	[57]
Mg-6Zn-1Ca	-	45.3	145	67	4.5	-	[57]

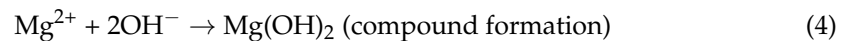
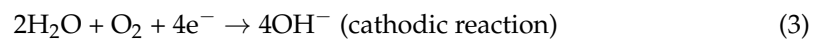
Compared with permanent metallic implants, the stress-shielding effect resulting from the stiffness/Young's modulus difference between implant and bone, which decreases the healing process, bone growth, and implant stability, can be reduced or even avoided by using Mg-based alloys.

Magnesium materials have Young's modulus around 40–45 GPa, which is similar to that of biological bone (5–30 GPa) and significantly lower than other permanent implant materials, such as stainless steel (195–205 GPa), Ti alloys (105–115 GPa), and Co–Cr alloys (230 GPa) [58,59]. Liu et al. [60] studied the yield tensile strength and ultimate

tensile strength of extruded Mg–4Zn alloys. They observed that with the increase in Ca and Mn addition, the microstructure has a more grain refinement process, with the presence of nanoscale secondary phase particles. Additionally, Liu et al. [60] found a Mg–4Zn–0.6Ca–0.7Mn alloy with a 320 MPa ultimate strength and 16% elongation.

### 3.3. Corrosion Resistance of Mg-Based Alloys

In many cases, biodegradable materials present the advantage that a second implant removal operation is not necessary, thus saving costs for the health system and offering benefits to the patient. The basic electrochemical character of magnesium, with a standard reduction potential ( $E^\circ$  (V)) =  $-2.375$  volts, conducts to low corrosion properties. Usually, the surface of magnesium implants passivates and creates a thin layer of magnesium oxide when exposed to air, preventing further chemical reactions. The corrosion process mechanism in different mediums (such as the biological environment) is presented by the reactions below [61].



Corrosion is an unwanted phenomenon in engineering applications, as it results in the degradation of material properties. Magnesium degradation, however, is correlated with the elimination of hydrogen, which can present problems in some biomedical applications. In Figure 8 is shown a schematic diagram of biocorrosion at the interface between Mg-based biomaterial and the biological medium.

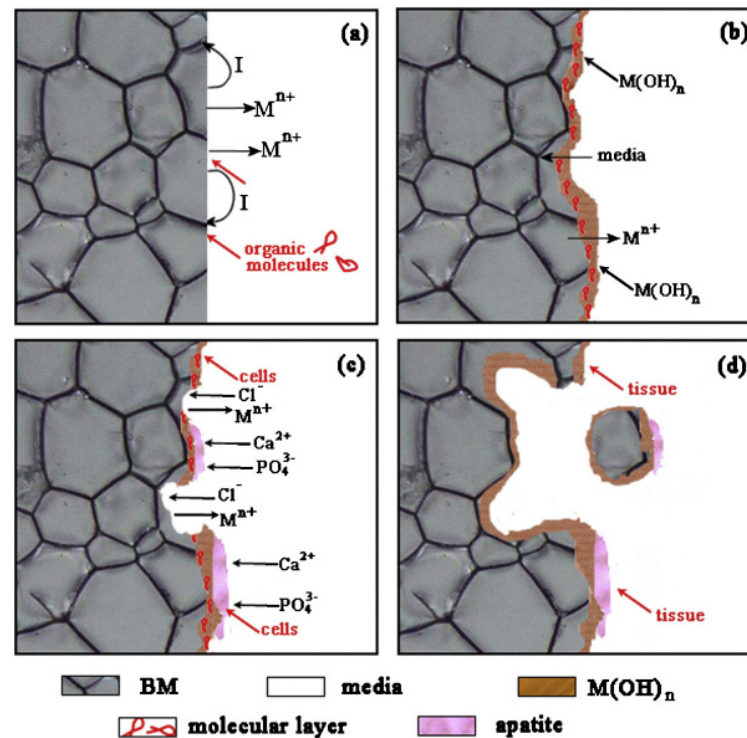


**Figure 8.** Schematic diagram of biocorrosion between Mg-based materials and the biological environment (adapted after [8]): (a) galvanic corrosion between the metal matrix and the intermetallic phase, or grain boundary; (b) beginning of biodegradable metal dissolution; (c) beginning of pitting corrosion; and (d) material degradation at the grain boundary.

The electrochemical evaluation of magnesium alloys explains their corrosion characteristics [62–66]. Zhang S. observed that the rate of corrosion using the immersion technique for pure Mg was 0.26 mm/year [67]. The most difficult aspect of corrosion testing is selecting the experimental environment. For these studies, it is essential to use solutions that replicate *in vivo* conditions as closely as feasible. Hank’s solution, simulated body fluid (SBF), Earle’s buffer (EBSS), and minimum essential medium (MEM) are the finest test medium. SBF’s ion content is very comparable to that of blood, but MEM includes glucose, amino acids, and vitamins [68]. Compared with blood, MEM and EBSS possess a somewhat lower concentration of Ca and Mg [69]. Numerous helpful effects might be achieved by using diverse circumstances. For pure Mg, the corrosion rate measured by immersion in EBSS and reported by Walker J. [70] was 0.39 mm/year, but it was 1.39 mm/year in SBF and 2.05 mm/year in Hank’s solutions. In addition, the rate of Mg degradation might rise from 0.25 mm/year in Hank’s solution to 1.88 mm/year in SBF [71]. Additionally, Song et al. evaluated the corrosion rate on Mg–0.25Ca–1Zn in a solution comprising 0.1 mol/L NaCl for 1 h and resulted in a 0.07 mm/year degradation [72].

The addition of more than 1 wt.% Zn at a constant calcium concentration of 0.5 or 1 wt.% resulted in a considerable decrease in corrosion rates compared with binary Mg–Ca, according to electrochemical analysis research [73]. In addition, other studies show that zinc concentrations over 2–3 wt.% lead to an increase in corrosion rates [74,75]. In Table 2 corrosion parameters of some Mg–Ca–Zn biodegradable alloys in HBSS immersion environment are presented.

**Table 2.** Corrosion parameters of some Mg–Ca–Zn biodegradable alloys [38,39].

Material	$E_{\text{corr}}$ (V)	$I_{\text{corr}}$ (A/cm <sup>2</sup> )	Immersion Environment	Ref.
Sample A—Mg–0.6Ca	−1.61	7.0	HBSS	[39]
Sample B—Mg–0.6Ca–0.8Zn	−1.74	3.5	HBSS	[39]
Sample C—Mg–0.6Ca–1.8Zn	−1.73	1.0	HBSS	[39]
Sample D—Mg–1.6Ca–0.8Zn	−1.72	5.0	HBSS	[39]
Sample E—Mg–1.6Ca–1.8Zn	−1.71	1.5	HBSS	[39]
Sample F—Mg–1.5Ca–1Zn	−1.62	4.4	HBSS	[38]
Sample G—Mg–0.5Ca–3Zn	−1.53	2.1	HBSS	[38]

Zhang et al. [57] performed electrochemical analysis on some Mg–xZn–1Ca biodegradable alloys ( $x = 0/1/2/3/4/5/6$  wt.%) in Hank’s solution. A first conclusion of Zhang’s research was that the corrosion potential of the Mg–xZn–1.0Ca alloys was higher than that of pure Mg and was correlated with Zn content. Mg–1Zn–1Ca and Mg–2Zn–1Ca alloys’ corrosion parameters were measured at −1557 and −1568 mV, which were similar to the values of pure magnesium. The Mg–5Zn–1Ca and Mg–6Zn–1Ca biodegradable alloys showed high electrochemical values between −1524 and −1547 mV, which were about 60 mV higher than that of pure Mg. The addition of Zn content improved the electrochemical parameters of the as-cast Mg–xZn–1Ca alloys and also influenced the current densities of the as-cast alloys in Hank’s solution. The reason for the increased corrosion potential of Mg–xZn–1Ca alloys was that the element Zn has high electronegativity. However, when the Zn content increased, the corrosion resistance was decreased [57].

Additionally, Zumdick et al. [76] studied the electrochemical behavior for Mg–0.6Ca–0.8Zn and Mg–0.6Ca–1.8Zn in artificial saliva of different compositions and observed a very low corrosion rate due to the lower Zn amount of the tested saliva and the influence of the artificial saliva chemistry. Therefore, studies showed that the mixture of mucin and urea served as corrosion inhibitors due to the formation of a homogeneous passive corrosion barrier layer.

Gong et al. [37] investigated the degradation process of some Mg–Ca–Zn alloys with Zn variance between 0 and 7.5 wt.% Zn. The morphological aspect of the surfaces immersed in a NaCl solution for 24 h is highlighted in Figure 9. They observed that after immersion, the surface of alloy b (Mg–0.8Ca–1.7Zn) was relatively compact. On the other hand, the surface of alloys a (Mg–0.8Ca), c (Mg–0.8–4.6Zn), and d (Mg–0.8–7.5Zn) showed corrosion

products on the whole surface and a more pronounced appearance of degradation. They concluded that the higher corrosion resistance of Zn-enriched  $Mg_2Ca$  leads to a uniform corrosion with a much lower degradation rate.

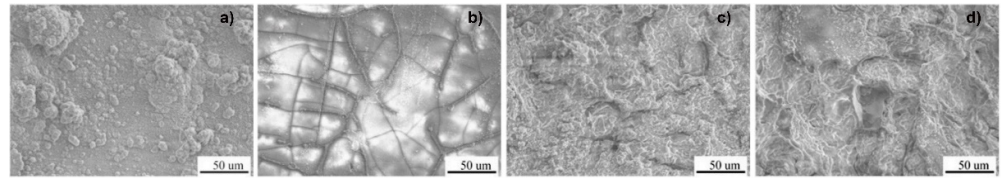


**Figure 9.** Morphological aspect of some Mg–Ca–Zn biodegradable alloys immersed in a NaCl solution for 24 h: (a) Mg–0.8Ca; (b) Mg–0.8Ca–1.7Zn; (c) Mg–0.8–4.6Zn; (d) Mg–0.8–7.5Zn [37].

After 24 h of immersion, the corrosion morphology in cross-section of the four alloys was described, confirming the study of the corrosion process. The  $Mg_2Ca$  phase dispersed along the grain border is corroded preferentially, causing grain loss and accelerated corrosion. The whole corrosion side of the Mg–0.8Ca–1.7Zn (alloy b) alloy is rather flat, suggesting homogeneous corrosion. The intermittent ternary phase forms a microgalvanic couple with the magnesium matrix, therefore increasing the corrosion of Mg–0.8–4.6Zn (alloy c) and Mg–0.8–7.5Zn (alloy d). Ultimately, the ternary phase of the network serves as a corrosion barrier to limit the progression of corrosion.

### 3.4. Biocompatibility of Biodegradable Alloys of the Mg–Ca–Zn System

The human body usually contains about 20–35 g magnesium/70 kg of body weight, and the daily requirement of this element is about 180–350 mg/day. In recent years, due to their biocompatibility and mechanical properties similar to biological bone, biodegradable magnesium-based alloys have been introduced as implants in orthopedic and trauma surgery [58]. Researchers are trying to develop biodegradable metals for various clinical applications, including their use in both the cardiovascular and orthopedic industries [40,77–79].

Previous studies have reported that magnesium shows good bone remodeling and biocompatibility [80,81], having a behavior that lends itself to use in fracture repair and healing as well as in reconstructive procedures requiring bone grafting. Thus, the mode of interaction of biodegradable materials in contact with the biological environment and implant response is schematically presented in Figure 10.

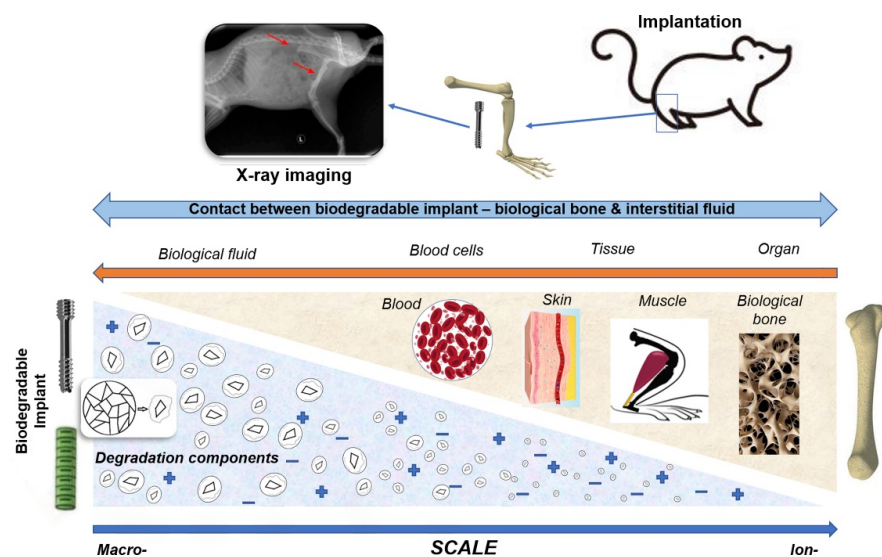


**Figure 10.** Mode of interaction of biodegradable materials in contact with the biological environment and implant response [82].

Recently, Mg–Ca–Zn alloys have been identified as promising candidates for orthopedic implantation due to their high strength, relatively low rate of degradation, and composition of critical human body components. Zhang et al. [15] found that the addition of 0.2% Ca significantly reduced approximately one-third of the degradation rate of cast Mg–4Zn alloy, while the degradation rate of cast Mg–4Zn–xCa alloy increased with increasing amounts of Ca ( $x = 0.2$ –2 wt.%), thereby significantly enhancing biocompatibility.

Other studies conducted by Li et al. [18] and Zhang et al. [57] revealed that Mg–1Ca alloys had good mechanical properties and biocompatibility among binary Mg–Ca alloys, and a content of 1–3 wt.% Zn increased biocompatibility between 80% and 95%.

The alloying elements of the Mg–Ca–Zn system have a different toxicological influence in the human body, and these aspects are presented in Table 3.

**Table 3.** Toxicological influence of Mg, Ca, and Zn in the human body used as alloying elements [83,84].

Element	Quantity in Human Body	Blood Level	Pathophysiology	Toxicology	Daily Necessary
Mg	25 g	0.73–1.06 mM	Activator of many enzymes; coregulator of protein synthesis and muscle contraction; stabilizer of DNA and RNA	Excess Mg leads to nausea	0.7 g
Ca	1100 g	0.919–0.993 mM	More than 99% is present in the skeleton structure; the rest of the Ca solution has a signal function, including muscle contraction, blood clotting, cell function, etc.	Inhibits intestinal absorption of other essential mineral	0.8 g
Zn	2 g	12.4–17.4 mM	Trace element; occurs in all classes of enzymes; most Zn occurs in the muscle	Neurotoxic and prevents bone formation and bone development at high concentration levels	15 mg

Bone remodeling is a very complex process, which demands a good correlation between multiple stem cells and a specific microenvironment. Many researchers have studied the effects of Mg-based biodegradable alloys on various kinds of osteogenic cells. Diaz-Tocados et al. [85] specified that increasing Mg ion concentrations (0.8, 1.2, and 1.8 mM) improves the osseointegration of mesenchymal stem cells (MSCs) in vitro. Additionally, Hung et al. [86] discovered that 10 mM Mg ion in the cell culture environment exhibits osteogenic differentiation of human mesenchymal stem cells derived from the bone marrow (BMSCs).

On the other hand, Bernardini et al. [87] studied that high-content Mg stimulates the proliferation and migration of microvascular cells. Other studies conducted by Li et al. [88] evaluated the effects of extracts of Mg–Zn–Mn alloy on the angiogenesis of human umbilical vein endothelial cells (HUVECs). The in vitro analysis showed that 6.25% Mg–Zn–Mn alloy extract induces the angiogenesis of HUVECs via the FGF signaling pathway, and Cho et al. [89] found that Mg–Ca–Zn alloy bone screws showed a faster degradation rate and better histopathological response than self-reinforced poly L-lactide (SR-PLLA).

Bone morphogenetic protein-2 (BMP-2), collagen-1 (Col-1), and Runx-2 are all indicators of osteogenesis, and Wang et al. [90] showed that Mg ions induced their expression in BMSCs through the MARK signaling pathway. The platelet-derived growth factor (PDGF) stimulates the growth and differentiation of osteoblasts, and its production and secretion were discovered to be facilitated by Mg in mouse embryo osteoblast precursor cells (MC<sub>3</sub>T<sub>3</sub>-E<sub>1</sub>) by Liu et al. [91]. Cell proliferation, adhesion, extracellular matrix (ECM) mineralization, and ALP activity were all enhanced in the Mg-coated Ti<sub>6</sub>Al<sub>4</sub>V coculture

with MC<sub>3</sub>T<sub>3</sub>-E<sub>1</sub> cells compared with the bare Ti<sub>6</sub>Al<sub>4</sub>V coculture, as was shown in a separate research by Gao et al. [92].

In addition, Mg enhanced the production of osteopontin, a gene critical for the first contact between biomaterials and cells throughout the osteogenic process, in adipose-derived stromal cells (ADSCs) [93]. The theoretical foundation for using Mg in the manufacture of orthopedic metal implants is that Mg may increase the osteogenic differentiation of diverse osteogenic cells. Bone regeneration relies heavily on the dynamic equilibrium between osteoclastogenesis and osteogenesis [94]. Magnesium (Mg) can control osteoblasts to stimulate bone regeneration and can also stop osteoclasts from breaking down the bone. By blocking the activation of the nuclear factor kappa B (NF-κB) and nuclear factor of activated T cells cytoplasmic 1 (NFATc1) signaling pathway, Zhai et al. [95] discovered that Mg leach liquor inhibited the activity of osteoclasts and prevented osteolysis in vivo. Further research by Wu et al. [96] showed that a Mg extract diluted to a 2 concentration in cell culture media both stimulated osteogenic development of osteoclasts and suppressed the differentiation of osteoclasts.

### 3.5. Potential Implant Application of Biodegradable Alloys of the Mg–Ca–Zn System

Magnesium alloys are considered the finest bioabsorbable metals for bone fracture repair implants. Absorbable magnesium alloys have a high rate of corrosion and degradation, which must be controlled. Several treatments have been developed for magnesium alloys to delay their corrosion rates down to the same level as the pace at which bone fractures heal. The rapid deterioration of metal due to corrosion is still a difficult problem to solve. Ideal implant characteristics include long-term biocompatibility, superior mechanical properties, and acceptable biodegradation rates. Base material and proper alloying element selection, alloying system selection (binary, ternary, quaternary, etc.), and respective compositions and microstructures (porous, composite, amorphous, etc.) are all crucial factors in optimizing these characteristics.

Clearly, the applications have a direct impact on the specifics of biodegradable materials' design and selection criteria. Orthopedic devices, such as screws, pins, needles, and plates, are placed into the bone to provide mechanical stability for 12–18 weeks while the bone heals [58]. Therefore, to avoid “stress shielding”, Mg-based alloys should have both high strength and a low modulus similar to the bone.

For biomaterials designed for bone fixtures, Erinc et al. [97] suggested a set of mechanical and corrosion parameters, including a corrosion rate of less than 0.5 mm year<sup>−1</sup> in simulated body fluid at 37 °C, a strength of more than 200 MPa, and an elongation of more than 10%. Another promising medical use for Mg-based alloys is the development of coronary stents, which are implanted to open blood channels and must work despite the constant movement caused by the blood.

In current industry trends, as stated by patients, magnesium-based screws have been utilized in clinical studies to heal/repair bone abnormalities without observable negative effects [98,99]. The most used temporary devices in orthopedic surgery are bone screws, interference screws, plates, nails, wires, pins, and scaffolds [9,100–103]. The first commercially available magnesium screws (Magnezix, Syntellix, Hannover, Germany) were accessible in 2013, and their removal 1 to 2 years after implantation was documented [104]. In addition, a new MgYREZr alloy interference bolt (Milagro, DePuy Mitek, Leeds, UK) was just launched to the market [105]. In animal investigations, magnesium alloy vascular stents with low corrosion rates were demonstrated to be mechanically viable for up to 6 months, and have since been assessed in human trials [106,107].

Recently, Shanghai Jiao Tong University [108] produced a new type of Mg–Nd–Zn-based alloy (Jiaoda BioMg, commonly known as JDBM) utilizing simulations of molecular dynamics and experimental data. Neodymium was chosen as the primary alloying element in this series of alloys, with Zn and Zr serving as microelements. Nd is one of the rare earth elements whose alloys (Mg–Nd binary alloys) have shown a considerable gain in mechanical characteristics [109] and a decrease in galvanic corrosion, although exhibiting some cytotoxic-

icity. Zn, one of the necessary dietary components in the human body, boosts the ductility and plasticity of the Mg alloy. JDBM-1 alloy was used to create bone plates, screws, and even 3D porous structures for bone tissue, whereas JDBM-2 alloy (with excellent ductility and moderate resistance) was used to create cardiovascular stents.

Initial clinical studies on magnesium alloys for clinical application revealed that they were excessively brittle, had inadequate mechanical features, and corroded extremely fast. Under the effect of technological innovations and new types of high-purity magnesium alloys with superior mechanical and corrosion performance, however, studies conducted by Heublein et al. between 2000 and 2003 [110] sparked interest in the medical applications of biodegradable magnesium-based alloys. Several orthopedic implants, including those not based on magnesium, are now in clinical use. Adsorbent metal stents (AMS) consisting of materials such as WE43 and modified Mg-based alloys and Magnezix-type screws are now employed in orthopedic applications [111,112]. Although significant progress has been achieved in recent years in the development of magnesium-based biodegradable alloys, medical applications still suffer a number of basic challenges.

Mg-based alloys have limited medical uses due to their high rate of disintegration and fast production (due to degradation) of hydrogen gas bubbles, frequently in the first week after surgery [113]. The basic research on bioresorbable metals focuses on three primary areas: (1) analysis of metal toxicity both in vitro and in vivo for the biocompatibility study, (2) improving the mechanical properties of metals by designing alloys (compositional) and by metallurgical processes, and (3) controlling corrosion behavior by modifying the substrate or surface with coatings or other surface treatments.

Good mechanical properties, a rapid-enough degradation rate, high biocompatibility and hemocompatibility rates, and the ability to transport drugs are all necessary for a biodegradable stent to be considered optimal. For the first 6–12 months, stent degradation is expected to be very slow to preserve the stent's mechanical integrity while the artery remodels. After that, degradation should proceed at a satisfactory pace without leading to an intolerable concentration of degradation products close to the implantation site. Eventually, stents should dissolve entirely within 12–24 months following implantation [114].

#### 4. Conclusions

Mg-based alloys are considered a new generation of biodegradable materials, which are mainly intended for the design of orthopedic implants. These alloys differ from other biomaterials due to their promising biodegradability in the physiological environment, which makes them suitable for the manufacture of various temporary orthopedic implants. It has been observed that these biodegradable materials possess a high degradation rate, which can lead to decreased mechanical strength. These constrictions can be reduced by proper selection of alloying elements with precise composition, resulting in microstructure refinement, improved surface characteristics, and manufacturing process.

The development of the Mg<sub>2</sub>Ca phase at the grain boundaries is caused by the addition of supersaturated Ca to a Mg-based alloy. Due to the production of thermally stable intermetallic phases, Ca can also improve the microstructure of magnesium and increase its strength, creep characteristics at high temperatures, and biocompatibility. The formation of a solid solution between Zn and Mg alloy enhances the alloy's mechanical characteristics. The ultimate tensile strength and elongation of as-cast Mg–Zn alloys increase significantly with a Zn component of up to 4 wt.%.

The enrichment of zinc in the solid solution of Mg–Ca–Zn alloys is thought to result in a decreased potential difference between the phases and, therefore, leads to the reduced corrosion rate of this alloy. For binary Mg–Ca, the high corrosion rates result from the dissolution of Mg<sub>2</sub>Ca at the grain boundary and the subsequent extraction of complete grains.

The in vitro degradation of Mg–Zn–Ca alloys indicated that zinc not only raised the corrosion potential of the magnesium alloys, but also increased their corrosion current. This was identified as a result of the reaction between zinc and magnesium. According to a variety of studies, the in vitro degradation rate of the Mg–Zn–Ca alloys with a high percentage

of zinc was much higher than that of high-purity magnesium when tested in Hank's solution. According to the results of in vitro cytotoxicity testing, Mg–Zn–Ca alloys with a composition of calcium between 0.5 and 1 wt.% and zinc between 1 and 4 wt.% did not induce toxicity in L-929 cells and are thus appropriate for use in biomedical applications.

Analyzing the studies conducted in this work from the perspectives of microstructural analysis, mechanical properties, electrochemical tests, and biocompatibility, we can estimate the optimal ratio of Ca in Mg–Ca–Zn alloys to be between 0.3 and 0.8 wt.% and the optimal ratio of Zn to be between 0.5 and 4 wt.%.

New research must be performed in the area of Mg–Ca–Zn alloys with a low rate of degradation and excellent mechanical characteristics. In addition, new Ca and Zn concentrations must be developed for these alloys to be more biocompatible. Due to the osseointegration characteristics of magnesium and its potential application for osseous defects produced by degenerative diseases or bone cancer healing in conjunction with biodegradable ceramics and polymers, these Mg–Ca–Zn alloys have enormous potential in the orthopedic domain.

**Author Contributions:** Conceptualization, B.I., C.M. and I.-V.A.; methodology, B.I.; software, B.I. and Ş.-C.L.; validation, C.M. and I.-V.A.; formal analysis, B.I. and Ş.-C.L.; investigation, B.I.; resources, B.I.; data curation, C.M. and I.-V.A.; writing—original draft preparation, B.I.; writing—review and editing, B.I., C.M. and I.-V.A.; visualization, Ş.-C.L.; supervision, C.M. and I.-V.A.; project administration, B.I.; funding acquisition, B.I. All authors have read and agreed to the published version of the manuscript.

**Funding:** This work was supported by a grant from the Ministry of Research, Innovation, and Digitization, CNCS—UEFISCDI, project number PN-III-P1-1.1-TE-2021-0702, within PNCDI III.

**Institutional Review Board Statement:** Not applicable.

**Informed Consent Statement:** Not applicable.

**Conflicts of Interest:** The authors declare no conflict of interest.

## References

1. Kulinetz, I. *Biomaterials and Their Applications in Medicine*. In *Regulatory Affairs for Biomaterials and Medical Devices*; Woodhead Publishing: Cambridge, UK, 2014; pp. 1–10; ISBN 978-085709920-4. [CrossRef]
2. Williams, D. *The Williams Dictionary of Biomaterials*; Liverpool University Press: Liverpool, UK, 1999; ISBN 978-0-85323-734-1.
3. Available online: <https://www.marketwatch.com/press-release/global-biomaterials-market-to-witness-a-cagr-of-144-during-2018-2024> (accessed on 30 August 2022).
4. Song, J.; Chen, J.; Xiong, X.; Peng, X.; Chen, D.; Pan, F. Research advances of magnesium and magnesium alloys worldwide in 2021. *J. Magnes. Alloy.* **2022**, *10*, 863–898. [CrossRef]
5. Hartwig, A. Role of magnesium in genomic stability. *Mutat. Res.* **2001**, *475*, 113–121. [CrossRef]
6. Manivasagam, G.; Suwas, S. Biodegradable Mg and Mg based alloys for biomedical implants. *Mater. Sci. Technol.* **2014**, *30*, 515–520. [CrossRef]
7. Purnama, A.; Hermawan, H.; Mantovani, D. Biodegradable metal stents: A focused review on materials and clinical studies. *J. Biomater. Tissue Eng.* **2014**, *4*, 868–874. [CrossRef]
8. Zheng, Y.F.; Gu, X.N.; Witte, F. Biodegradable metals. *Mater. Sci. Eng. R Rep.* **2014**, *77*, 1–34. [CrossRef]
9. Antoniac, I.; Miculescu, M.; Manescu, V.; Stere, A.; Quan, P.H.; Paltanea, G.; Robu, A.; Earar, K. Magnesium-Based Alloys Used in Orthopedic Surgery. *Materials* **2022**, *15*, 1148. [CrossRef] [PubMed]
10. Tsakiris, V.; Tardei, C.; Clicinschi, F.M. Biodegradable Mg alloys for orthopedic implants—A review. *J. Magnes. Alloy.* **2021**, *9*, 1884–1905. [CrossRef]
11. Kirkland, N.; Staiger, M.; Nisbet, D.; Davies, C.J.; Birbilis, N. Performance-Driven Design of Biocompatible Mg Alloys. *JOM* **2011**, *63*, 28–34. [CrossRef]
12. Lopes de Oliveira, M.C.; Marques Pereira, V.S.; Correa, O.V.; Antunes, R.A. Corrosion Performance of Anodized AZ91D Magnesium Alloy: Effect of the Anodizing Potential on the Film Structure and Corrosion Behavior. *J. Mater. Eng. Perform.* **2014**, *23*, 593–603. [CrossRef]
13. Cai, S.; Lei, T.; Li, N.; Feng, F. Effects of Zn on microstructure, mechanical properties and corrosion behavior of Mg–Zn alloys. *Mater. Sci. Eng. C* **2012**, *32*, 2570–2577. [CrossRef]
14. Avedesian, M.M.; Baker, H. *Magnesium and Magnesium Alloys*; ASM International: Materials Park, OH, USA, 1999; pp. 106–118; ISBN 978-0-87170-657-7.

15. Zhang, B.P.; Wang, Y.; Geng, L. Research on Mg–Zn–Ca alloy as degradable biomaterial. *Biomater. Phys. Chem. Z. Tech.* **2011**, *183*–204. [[CrossRef](#)]
16. Xu, Z.G.; Smith, C.; Chen, S.O.; Sankar, J. Development and microstructural characterizations of Mg–Zn–Ca alloys for biomedical applications. *Mater. Sci. Eng. B Adv.* **2011**, *176*, 1660–1665. [[CrossRef](#)]
17. Smith, C.E.; Xu, Z.; Waterman, J.; Sankar, J. Cytocompatibility assessment of MgZnCa alloys. *Emerg. Mater. Res.* **2013**, *2*, 283–290. [[CrossRef](#)]
18. Li, Z.; Gu, X.; Lou, S.; Zheng, Y. The development of binary Mg–Ca alloys for use as biodegradable materials within bone. *Biomaterials* **2008**, *29*, 1329–1344. [[CrossRef](#)] [[PubMed](#)]
19. Ibrahim, H.; Klarnar, A.D.; Poorganji, B.; Dean, D.; Luo, A.A.; Elahinia, M. Microstructural, mechanical and corrosion characteristics of heat-treated Mg-1.2Zn-0.5Ca (wt.%) alloy for use as resorbable bone fixation material. *J. Mech. Behav. Biomed. Mater.* **2017**, *69*, 203–212. [[CrossRef](#)]
20. Jung, Y.G.; Yang, W.; Kim, Y.J.; Kim, S.K.; Yoon, Y.O.; Lim, H.; Kim, D.H. Effect of Ca addition on the microstructure and mechanical properties of heat-treated Mg-6.0Zn-1.2Y-0.7Zr alloy. *J. Magnes. Alloy.* **2021**, *9*, 1619–1631. [[CrossRef](#)]
21. Witte, F.; Hort, N.; Vogt, C.; Cohen, S.; Kainer, K.U.; Willumeit, R.; Feyerabend, F. Degradable biomaterials based on magnesium corrosion. *Curr. Opin. Solid State Mater. Sci.* **2008**, *12*, 63–72. [[CrossRef](#)]
22. Bairagi, D.; Mandal, S. A comprehensive review on biocompatible Mg-based alloys as temporary orthopaedic implants: Current status, challenges, and future prospects. *J. Magnes. Alloy.* **2022**, *10*, 627–669. [[CrossRef](#)]
23. Jin, Z.Z.; Zha, M.; Wang, S.Q.; Wang, S.C.; Wang, C.; Jia, H.L.; Wang, H.Y. Alloying design and microstructural control strategies towards developing Mg alloys with enhanced ductility. *J. Magnes. Alloy.* **2022**, *10*, 1191–1206. [[CrossRef](#)]
24. Tipan, N.; Pandey, A.; Mishra, P. Selection and preparation strategies of Mg-alloys and other biodegradable materials for orthopaedic applications: A review. *Mater. Today Commun.* **2022**, *31*, 103658. [[CrossRef](#)]
25. Chen, J.; Tan, L.; Yu, X.; Etim, I.P.; Ibrahim, M.; Yang, K. Mechanical properties of magnesium alloys for medical application: A review. *J. Mech. Behav. Biomed. Mater.* **2018**, *87*, 68–79. [[CrossRef](#)] [[PubMed](#)]
26. Rahim, S.A.; Muhammad Rabeeh, V.P.; Joseph, M.A.; Hanas, T. Does acid pickling of Mg-Ca alloy enhance biomineralization? *J. Magnes. Alloy.* **2021**, *9*, 1028–1038. [[CrossRef](#)]
27. Nidadavolu, E.P.S.; Krüger, D.; Zeller-Plumhoff, B.; Tolnai, D.; Wiese, B.; Feyerabend, F.; Ebel, T.; Willumeit-Römer, R. Pore characterization of PM Mg–0.6Ca alloy and its degradation behavior under physiological conditions. *J. Magnes. Alloy.* **2021**, *9*, 686–703. [[CrossRef](#)]
28. McCall, K.A.; Huang, C.; Fierke, C.A. Function and mechanism of zinc metalloenzymes. *J. Nutr.* **2000**, *130*, 1437–1446. [[CrossRef](#)]
29. Tapiero, H.; Tew, K.D. Trace elements in human physiology and pathology: Zinc and metallothioneins. *Biomed. Pharmacother.* **2003**, *57*, 399–411. [[CrossRef](#)]
30. Sezer, N.; Evis, Z.; Koç, M. Additive manufacturing of biodegradable magnesium implants and scaffolds: Review of the recent advances and research trends. *J. Magnes. Alloy.* **2021**, *9*, 392–415. [[CrossRef](#)]
31. Merson, D.; Brilevsky, A.; Myagkikh, P.; Tarkova, A.; Prokhorikhin, A.; Kretov, E.; Frolova, T.; Vinogradov, A. The functional properties of Mg–Zn–X biodegradable magnesium alloys. *Materials* **2020**, *13*, 544. [[CrossRef](#)]
32. Bazhenova, V.E.; Li, A.V.; Komissarov, A.A.; Koltygin, A.V.; Tavolzhanskii, S.A.; Bautin, V.A.; Voropaeva, O.O.; Mukhametshin, A.M.; Tokar, A.A. Microstructure and mechanical and corrosion properties of hot-extruded Mg–Zn–Ca–(Mn) biodegradable alloys. *J. Magnes. Alloy.* **2021**, *9*, 1428–1442. [[CrossRef](#)]
33. Wasiur-Rahman, S.; Medraj, M. Critical assessment and thermodynamic modeling of the binary Mg–Zn, Ca–Zn and ternary Mg–Ca–Zn systems. *Intermetallics* **2009**, *17*, 847–864. [[CrossRef](#)]
34. Paris, R. Ternary alloys. No. 45. Publications Scientifiques et Techniques du minist'ere de L'Air. *Ministère L'Air* **1934**, *45*, 1–86.
35. Clark, J.B. The solid constitution in the Mg-rich region of the Mg–Ca–Zn phase diagram. *Trans. Metall. Soc. AIME* **1961**, *221*, 644–645.
36. Zander, D.; Zumdick, N.A. Influence of Ca and Zn on the microstructure and corrosion of biodegradable Mg–Ca–Zn alloys. *Corros. Sci.* **2015**, *93*, 222–233. [[CrossRef](#)]
37. Gong, C.; He, X.; Yan, X. Corrosion behavior of Mg–Ca–Zn alloys with high Zn content. *J. Phys. Chem. Solids* **2021**, *152*, 109952. [[CrossRef](#)]
38. Zhang, E.; Yang, L. Microstructure, mechanical properties and bio-corrosion properties of Mg–Zn–Mn–Ca alloy for biomedical application. *Mater. Sci. Eng. A* **2008**, *497*, 111–118. [[CrossRef](#)]
39. Pulido-González, N.; Hidalgo-Manrique, P.; García-Rodríguez, S.; Torres, B.; Rams, J. Effect of heat treatment on the mechanical and biocorrosion behaviour of two Mg–Zn–Ca alloys. *J. Magnes. Alloy.* **2022**, *10*, 540–554. [[CrossRef](#)]
40. Bitá, A.I.; Antoniac, I.; Miculescu, M.; Stan, G.E.; Leonat, L.; Antoniac, A.; Constantin, B.; Forná, N. Electrochemical and In Vitro Biological Evaluation of Bio-Active Coatings Deposited by Magnetron Sputtering onto Biocompatible Mg-0.8Ca Alloy. *Materials* **2022**, *15*, 3100. [[CrossRef](#)]
41. Baltatu, I.; Sandu, A.V.; Baltatu, M.S.; Benchea, M.; Achitei, D.C.; Ciolacu, F.; Perju, M.C.; Vizureanu, P.; Benea, L. Structural and Physical characterization of new Ti–Ba–Sed alloyS. *Arch. Metall. Mater.* **2022**, *67*, 255–259.
42. Baltatu, M.S.; Spataru, M.C.; Verestiuc, L.; Balan, V.; Solcan, C.; Sandu, A.V.; Geanta, V.; Voiculescu, I.; Vizureanu, P. Design, Synthesis, and Preliminary Evaluation for Ti–Mo–Zr–Ta–Si Alloys for Potential Implant Applications. *Materials* **2021**, *14*, 6806. [[CrossRef](#)]

43. Wei, S.; Ma, J.X.; Xu, L.; Gu, X.S.; Ma, X.L. Biodegradable materials for bone defect repair. *Mil. Med. Res.* **2020**, *7*, 1–25. [CrossRef]
44. Rho, J. Democratic science. *Nature* **1974**, *251*, 673.
45. Chandra, G.; Pandey, A. Preparation Strategies for Mg-alloys for biodegradable orthopedic implants and other biomedical applications: A review. *IRBM* **2020**, *43*, 229–249.
46. Available online: <https://material-properties.org/calcium-mechanical-properties-strength-hardness-crystal-structure/> (accessed on 30 August 2022).
47. Sotoudeh Bagha, P.; Khaleghpanah, S.; Sheibani, S.; Khakbiz, M.; Zakeri, A. Characterization of nanostructured biodegradable Zn-Mn alloy synthesized by mechanical alloying. *J. Alloy. Compd.* **2018**, *735*, 1319–1327. [CrossRef]
48. Menthe, E.; Bulak, A.; Olfe, J.; Zimmermann, A.; Rie, K.T. Improvement of the mechanical properties of austenitic stainless steel after plasma nitriding. *Surf. Coat Technol.* **2000**, *133–134*, 259–263. [CrossRef]
49. Kuo, C.K.; Ma, P.X. Ionically crosslinked alginate hydrogels as scaffolds for tissue engineering: Part 1. Structure, gelation rate and mechanical properties. *Biomaterials* **2001**, *22*, 511–521. [CrossRef]
50. Bridgeport, D.A.; Brantley, W.A.; Herman, P.F. Cobalt-Chromium and Nickel Chromium alloys for removable prosthodontics, Part 1: Mechanical properties. *J. Prosthodont. Sep.* **1993**, *2*, 144–150. [CrossRef]
51. Seong, J.W.; Kim, W.J. Development of biodegradable Mg–Ca alloy sheets with enhanced strength and corrosion properties through the refinement and uniform dispersion of the Mg<sub>2</sub>Ca phase by high-ratio differential speed rolling. *Acta Biomater.* **2015**, *11*, 531–542. [CrossRef]
52. Gu, X.; Zheng, Y.; Zhong, S.; Xi, T.; Wang, J.; Wang, W. Corrosion of, and cellular responses to Mg-Zn-Ca bulk metallic glasses. *Biomaterials* **2010**, *31*, 1093–1103. [CrossRef]
53. Razzaghi, M.; Kasiri-Asgarani, M.; Bakhsheshi-Rad, H.R.; Ghayour, H. Microstructure, mechanical properties, and in-vitro biocompatibility of nanoNiTi reinforced Mg–3Zn–0.5Ag alloy: Prepared by mechanical alloying for implant applications. *Compos. Part B Eng.* **2020**, 107947. [CrossRef]
54. Abdel-Gawad, S.A.; Shoeib, M.A. Corrosion Studies and Microstructure of Mg–Zn–Ca Alloys for Biomedical Applications. *Surf. Interfaces* **2019**, *14*, 108–116. [CrossRef]
55. Duley, P.; Sanyal, S.; Bandyopadhyay, T.K.; Mandal, S. Homogenization-Induced Age-Hardening Behavior and Room Temperature Mechanical Properties of Mg–4Zn–0.5Ca–0.16Mn (wt.%). *Alloy. Mater. Design* **2019**, *164*, 107554. [CrossRef]
56. González, S.; Pellicer, E.; Fornell, J.; Blanquer, A.; Barrios, L.; Ibáñez, E.; Solsona, P.; Suriñach, S.; Baró, M.D.; Nogués, C.; et al. Improved mechanical performance and delayed corrosion phenomena in biodegradable Mg–Zn–Ca alloys through Pd-alloying. *J. Mech. Behav. Biomed. Mater.* **2011**, *6*, 53–62. [CrossRef] [PubMed]
57. Zhang, B.; Hou, Y.; Wang, X.; Wang, Y.; Geng, L. Mechanical properties, degradation performance and cytotoxicity of Mg–Zn–Ca biomedical alloys with different compositions. *Mater. Sci. Eng. C* **2011**, *31*, 1667–1673. [CrossRef]
58. Staiger, M.P.; Pietak, A.M.; Huadmai, J.; Dias, G. Magnesium and its alloys as orthopedic biomaterials: A review. *Biomaterials* **2006**, *27*, 1728–1734. [CrossRef] [PubMed]
59. Antoniac, I.; Sinescu, C.; Antoniac, A. Adhesion aspects in biomaterials and medical devices. *J. Adhes. Sci. Technol.* **2016**, *30*, 1711–1715.
60. Liu, C.; Chen, X.; Chen, J.; Atrens, A.; Pan, F. The effects of Ca and Mn on the microstructure, texture and mechanical properties of Mg–4 Zn alloy. *J. Magnes. Alloy.* **2021**, *9*, 1084–1097. [CrossRef]
61. Somekawa, H.; Mukai, T. High strength and fracture toughness balance on the extruded Mg–Ca–Zn alloy. *Mater. Sci. Eng. A* **2007**, *459*, 366–370. [CrossRef]
62. Antoniac, I.; Miculescu, F.; Cotrut, C.; Fica, A.; Rau, J.V.; Grosu, E.; Antoniac, A.; Tecu, C.; Cristescu, I. Controlling the Degradation Rate of Biodegradable Mg–Zn–Mn Alloys for Orthopedic Applications by Electrophoretic Deposition of Hydroxyapatite Coating. *Materials* **2020**, *13*, 263. [CrossRef]
63. Rau, J.V.; Antoniac, I.; Filipescu, M.; Cotrut, C.; Fosca, M.; Nistor, L.C.; Birjega, R.; Dinescu, M. Hydroxyapatite Coatings on Mg–Ca Alloy Prepared by Pulsed Laser Deposition: Properties and Corrosion Resistance in Simulated Body Fluid. *Ceram. Int.* **2018**, *44*, 16678–16687. [CrossRef]
64. Mareci, D.; Bolat, G.; Izquierdo, J.; Crimu, C.; Munteanu, C.; Antoniac, I.; Souto, R.M. Electrochemical Characteristics of Bioresorbable Binary MgCa Alloys in Ringer’s Solution: Revealing the Impact of Local PH Distributions during in-Vitro Dissolution. *Mater. Sci. Eng. C* **2016**, *60*, 402–410. [CrossRef]
65. Antoniac, I.; Adam, R.; Biță, A.; Miculescu, M.; Trante, O.; Petrescu, I.M.; Pogărașteanu, M. Comparative Assessment of In Vitro and In Vivo Biodegradation of Mg–1Ca Magnesium Alloys for Orthopedic Applications. *Materials* **2020**, *14*, 84. [CrossRef] [PubMed]
66. Antoniac, I.V.; Antoniac, A.; Vasile, E.; Tecu, C.; Fosca, M.; Yankova, V.G.; Rau, J.V. In Vitro Characterization of Novel Nanostructured Collagen-Hydroxyapatite Composite Scaffolds Doped with Magnesium with Improved Biodegradation Rate for Hard Tissue Regeneration. *Bioact. Mater.* **2021**, *6*, 3383–3395. [CrossRef] [PubMed]
67. Zhang, Y.F.; Hinton, B.; Wallace, G.; Liu, X.; Forsyth, M. On corrosion behaviour of magnesium alloy AZ31 in simulated body fluids and influence of ionic liquid pretreatments. *Corros. Eng. Sci. Technol.* **2012**, *47*, 374–382. [CrossRef]
68. Agha, N.A.; Feyerabend, F.; Mihailova, B.; Heidrich, S.; Bismayer, U.; Willumeit-Römer, R. Magnesium degradation influenced by buffering salts in concentrations typical of in vitro and in vivo models. *Mater. Sci. Eng. C* **2016**, *58*, 817–825. [CrossRef]

69. Marco, I.; Myrissa, A.; Martinelli, E.; Feyerabend, F.; Willumeit-Römer, R.; Weinberg, A.; Van der Biest, O. In vivo and in vitro degradation comparison of pure Mg, Mg-10Gd and Mg-2Ag: A short-term study. *Eur. Cells Mater.* **2017**, *33*, 90–104. [[CrossRef](#)] [[PubMed](#)]
70. Walker, J.; Shadanbaz, S.; Kirkland, N.T.; Stace, E.; Woodfield, T.; Staiger, M.P.; Dias, G.J. Magnesium alloys: Predicting in vivo corrosion with in vitro immersion testing. *J. Biomed. Mater. Res.* **2012**, *100*, 1134–1141. [[CrossRef](#)]
71. Marco, I.; Feyerabend, F.; Willumeit-Römer, R.; Van der Biest, O. Influence of testing environment on the degradation behavior of magnesium alloys for bioabsorbable implants. In Proceedings of the 144th Annual Meeting & Exhibition: Supplemental 2015, Orlando, FL, USA, 15–19 March 2015; pp. 499–506.
72. Song, J.; Gao, Y.; Liu, C.; Chen, Z. The effect of Sr addition on the microstructure and corrosion behaviour of a Mg-Zn-Ca alloy. *Surf. Coat. Technol.* **2022**, *437*, 128328. [[CrossRef](#)]
73. Bornapour, M.; Celikin, M.; Pekguleryuz, M. Thermal exposure effects on the in vitro degradation and mechanical properties of Mg-Sr and Mg-Ca-Sr biodegradable implant alloys and the role of the microstructure. *Mater. Sci. Eng. C* **2015**, *46*, 16–24. [[CrossRef](#)] [[PubMed](#)]
74. Du, H.; Wei, Z.; Liu, X.; Zhang, E. Effects of Zn on the microstructure, mechanical property and bio-corrosion property of Mg-3Ca alloys for biomedical application. *Mater. Chem. Phys.* **2011**, *125*, 568–575. [[CrossRef](#)]
75. Song, Y.; Han, E.H.; Shan, D.; Yim, C.D.; You, B.S. The effect of Zn concentration on the corrosion behavior of Mg-xZn alloys. *Corros. Sci.* **2012**, *65*, 322–330. [[CrossRef](#)]
76. Zumdick, N.; Ubbler, S.; Modabber, A.; Goloborodko, E.; Neuß-Stein, S.; Zander, D. Corrosion behavior of Mg-Ca-Zn alloys in artificial saliva. *Eur. Cell Mater.* **2015**, *30*, 49.
77. Adam, R.; Antoniac, I.; Avram, G.M.; Niculescu, M. Mg-1Ca alloy intramedullary nailing influence on bone callus formation and on vital organs functions, as an alternative to bioplastics. *Rom. J. Mil. Med.* **2022**, *125*, 31–41. [[CrossRef](#)]
78. Xing, F.; Li, S.; Yin, D.; Xie, J.; Rommens, P.M.; Xiang, Z.; Liu, M.; Ritz, U. Recent progress in Mg-based alloys as a novel bioabsorbable biomaterials for orthopedic applications. *J. Magnes. Alloy.* **2022**, *10*, 1428–1456. [[CrossRef](#)]
79. Wang, J.; Dou, J.; Wang, Z.; Hu, C.; Yu, H.; Chen, C. Research progress of biodegradable magnesium-based biomedical materials: A review. *J. Alloy. Compd.* **2022**, *923*, 166377. [[CrossRef](#)]
80. Witte, F.; Kaese, V.; Haferkamp, H.; Switzer, E.; Meyer-Lindenberg, A.; Wirth, C.J.; Windhagen, H. In vivo corrosion of four magnesium alloys and the associated bone response. *Biomaterials* **2005**, *26*, 3557–3563. [[CrossRef](#)]
81. Quan, P.H.; Antoniac, I.; Miculescu, F.; Antoniac, A.; Manescu, V.; Robu, A.; Bitu, A.I.; Miculescu, M.; Saceleanu, A.; Bodog, A.D.; et al. Fluoride Treatment and In Vitro Corrosion Behavior of Mg-Nd-Y-Zn-Zr Alloys Type. *Materials* **2022**, *15*, 566. [[CrossRef](#)] [[PubMed](#)]
82. Chin, P.Y.Y.; Cheok, Q.; Glowacz, A.; Caesarendra, W. A Review of In-Vivo and In-Vitro Real-Time Corrosion Monitoring Systems of Biodegradable Metal Implants. *Appl. Sci.* **2020**, *10*, 3141. [[CrossRef](#)]
83. Seiler, H.G.; Sigel, H. *Handbook of Toxicity of Inorganic Compounds*; Marcel Dekker Inc.: New York, NY, USA, 1988.
84. Sigel, H. *Metal Ions in Biological System*; Marcel Dekker Inc.: New York, NY, USA, 1986.
85. López, H.Y.; Cortés-Hernández, D.A.; Escobedo, S.; Mantovani, D. In Vitro Bioactivity Assessment of Metallic Magnesium. *Key Eng. Mater.* **2006**, *309–311*, 453–456. [[CrossRef](#)]
86. Hung, C.C.; Chaya, A.; Liu, K.; Verdelis, K.; Sfeir, C. The role of magnesium ions in bone regeneration involves the canonical Wnt signaling pathway. *Acta Biomater.* **2019**, *98*, 246–255. [[CrossRef](#)]
87. Bernardini, D.; Nasulewicz, A.; Mazur, A.; Maier, J.A. Magnesium and microvascular endothelial cells: A role in inflammation and angiogenesis. *Front. Biosci.* **2005**, *10*, 1177–1182. [[CrossRef](#)]
88. Li, D.; Yuan, Q.; Yu, K.; Xiao, T.; Liu, L.; Dai, Y.; Xiong, L.; Zhang, B.; Li, A. Mg-Zn-Mn alloy extract induces the angiogenesis of human umbilical vein endothelial cells via FGF/FGFR signaling pathway. *Biochem. Biophys. Res. Commun.* **2019**, *514*, 618–624. [[CrossRef](#)] [[PubMed](#)]
89. Cho, S.Y.; Chae, S.W.; Choi, K.W.; Seok, H.K.; Kim, Y.C.; Jung, J.Y.; Yang, S.J.; Kwon, G.J.; Kim, J.T.; Assad, M. Biocompatibility and strength retention of biodegradable Mg-Ca-Zn alloy bone implants. *J. Biomed. Mater. Res. B Appl. Biomater.* **2013**, *101B*, 201–212. [[CrossRef](#)] [[PubMed](#)]
90. Wang, Z.; Liu, Q.; Liu, C.; Tan, W.; Tang, M.; Zhou, X.; Sun, T.; Deng, Y. Mg<sup>2+</sup> in  $\beta$ -TCP/Mg-Zn composite enhances the differentiation of human bone marrow stromal cells into osteoblasts through MAPK-regulated Runx2/Osx. *J. Cell. Physiol.* **2020**, *235*, 5182–5191. [[CrossRef](#)]
91. Liu, W.; Guo, S.; Tang, Z.; Wei, X.; Gao, P.; Wang, N.; Li, X.; Guo, Z. Magnesium promotes bone formation and angiogenesis by enhancing MC3T3-E1 secretion of PDGF-BB. *Biochem. Biophys. Res. Commun.* **2020**, *528*, 664–670. [[CrossRef](#)]
92. Gao, P.; Fan, B.; Yu, X.; Liu, W.; Wu, J.; Shi, L.; Yang, D.; Tan, L.; Wan, P.; Hao, Y.; et al. Biofunctional magnesium coated Ti6Al4V scaffold enhances osteogenesis and angiogenesis in vitro and in vivo for orthopedic application. *Bioact. Mater.* **2020**, *5*, 680–693. [[CrossRef](#)]
93. Cecchinato, F.; Karlsson, J.; Ferroni, L.; Gardin, C.; Galli, S.; Wennerberg, A.; Zavan, B.; Andersson, M.; Jimbo, R. Osteogenic potential of human adipose-derived stromal cells on 3-dimensional mesoporous TiO<sub>2</sub> coating with magnesium impregnation. *Mater. Sci. Eng. C* **2015**, *52*, 225–234. [[CrossRef](#)] [[PubMed](#)]
94. El-Rashidy, A.A.; Roether, J.A.; Harhaus, L.; Kneser, U.; Boccaccini, A.R. Regenerating bone with bioactive glass scaffolds: A review of in vivo studies in bone defect models. *Acta Biomater.* **2017**, *62*, 1–28. [[CrossRef](#)]

95. Zhai, Z.; Qu, X.; Li, H.; Yang, K.; Wan, P.; Tan, L.; Ouyang, Z.; Liu, X.; Tian, B.; Xiao, F.; et al. The effect of metallic magnesium degradation products on osteoclast-induced osteolysis and attenuation of NF- $\kappa$ B and NFATc1 signaling. *Biomaterials* **2014**, *35*, 6299–6310. [CrossRef]
96. Wu, L.; Feyerabend, F.; Schilling, A.F.; Willumeit-Römer, R.; Luthringer, B.J.C. Effects of extracellular magnesium extract on the proliferation and differentiation of human osteoblasts and osteoclasts in coculture. *Acta Biomater.* **2015**, *27*, 294–304. [CrossRef]
97. Erinc, M.; Sillekens, W.H.; Mannens, R.; Werkhoven, R.J. Applicability of existing magnesium alloys as biomedical implant materials. *Magnes. Technol.* **2009**, 209–214. Available online: <https://www.narcis.nl/publication/RecordID/oa:tudelft.nl:uuid%3A4872dafb-0680-47c0-8751-bdce953b4cfe> (accessed on 30 August 2022).
98. Seitz, J.-M.; Lucas, A.; Kirschner, M. Magnesium-Based Compression Screws: A Novelty in the Clinical Use of Implants. *JOM* **2016**, *68*, 1177–1182. [CrossRef]
99. Plaass, C.; Von Falck, C.; Ettinger, S.; Sonnow, L.; Calderone, F.; Weizbauer, A.; Reifenrath, J.; Claassen, L.; Waizy, H.; Daniilidis, K.; et al. Bioabsorbable magnesium versus standard titanium compression screws for fixation of distal metatarsal osteotomies –3 year results of a randomized clinical trial. *J. Orthop. Sci.* **2018**, *23*, 321–327. [CrossRef]
100. Adam, R.; Gheorghiu, N.; Orban, H.; Antoniac, I.; Barbilian, A. Evolution toward New Bioabsorbable Material for Osteosynthesis Implants Used in Foot and Ankle Surgery. *Arch. Balk. Med. Union* **2016**, *51*, 190–198.
101. Pins-Syntellix, AG. Available online: <https://www.syntellix.de/en/products/advantages-and-application/pins.html> (accessed on 7 December 2021).
102. Resoloy®: A Magnesium Alloy for Absorbable Devices-Fort Wayne Metals. Available online: <https://www.fwmetals.com/services/r-d/rd-update/previous-rd-updates/resoloy-a-magnesium-alloy-for-absorbable-devices/> (accessed on 16 October 2021).
103. All-Syntellix AG. Available online: <https://www.syntellix.de/en/products/product-overview/all.html> (accessed on 16 October 2021).
104. Windhagen, H.; Radtke, K.; Weizbauer, A.; Diekmann, J.; Noll, Y.; Kreimeyer, U.; Schavan, R.; Stukenborg-Colsman, C.; Waizy, H. Biodegradable magnesium-based screw clinically equivalent to titanium screw in hallux valgus surgery: Short term results of the first prospective, randomized, controlled clinical pilot study. *Biomed. Eng.* **2013**, *12*, 62. [CrossRef] [PubMed]
105. Ezechieli, M.; Meyer, H.; Lucas, A.; Helmecke, P.; Becher, C.; Calliess, T.; Windhagen, H.; Ettinger, M. Biomechanical Properties of a Novel Biodegradable Magnesium-Based Interference Screw. *Orthop. Rev.* **2016**, *8*, 6445. [CrossRef] [PubMed]
106. Ang, H.Y.; Huang, Y.Y.; Lim, S.T.; Joner, M.; Wong, P.; Foin, N. Mechanical behavior of polymer-based vs. metallic-based bioresorbable stents. *J. Thorac. Dis.* **2017**, *9*, S923–S934. [CrossRef]
107. Erbel, R.; Di Mario, C.; Bartunek, J.; Bonnier, J.; De Bruyne, B.; Eberli, F.R.; Erne, P.; Haude, M.; Heublein, B.; Horrigan, M.; et al. Temporary scaffolding of coronary arteries with bioabsorbable magnesium stents: A prospective, non-randomised multicentre trial. *Lancet N. Am. Ed.* **2007**, *369*, 1869–1875. [CrossRef]
108. Zhang, X.; Yuan, G.; Mao, L.; Niu, J.; Ding, W. Biocorrosion properties of as-extruded Mg–Nd–Zn–Zr alloy compared with commercial AZ31 and WE43 alloys. *Mater. Lett.* **2012**, *66*, 209–211. [CrossRef]
109. Willbold, E.; Weizbauer, A.; Loos, A.; Seitz, J.M.; Angrisani, N.; Windhagen, H.; Reifenrath, J. Magnesium alloys: A stony pathway from intensive research to clinical reality. Different test methods and approval-related considerations. *J. Biomed Mater. Res. A* **2017**, *105*, 329–347. [CrossRef]
110. Heublein, B.; Rohde, R.; Kaese, V.; Niemeyer, M.; Hartung, W.; Haverich, A. Biocorrosion of magnesium alloys: A new principle in cardiovascular implant technology? *Heart* **2003**, *89*, 651–656. [CrossRef]
111. Hermawan, H. Updates on the research and development of absorbable metals for biomedical applications. *Prog. Biomater.* **2018**, *7*, 93–110. [CrossRef]
112. Ding, W. Opportunities and challenges for the biodegradable magnesium alloys as next-generation biomaterials. *Regen. Biomater.* **2016**, *3*, 79–86. [CrossRef]
113. Hermawan, H. *Biodegradable Metals: State of the Art*; Springer: Berlin/Heidelberg, Germany, 2012.
114. Hermawan, H.; Dubé, D.; Mantovani, D. Developments in metallic biodegradable stents. *Acta Biomater.* **2010**, *6*, 1693–1697. [CrossRef] [PubMed]